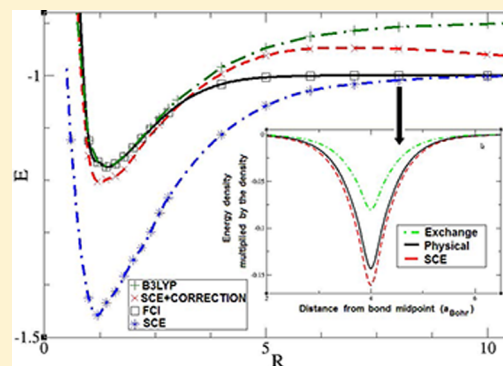


# Hydrogen Molecule Dissociation Curve with Functionals Based on the Strictly Correlated Regime

Stefan Vuckovic, Lucas O. Wagner, André Mirtschink, and Paola Gori-Giorgi\*

Department of Theoretical Chemistry and Amsterdam Center for Multiscale Modeling, FEW, Vrije Universiteit, De Boelelaan 1083, 1081HV Amsterdam, The Netherlands

**ABSTRACT:** Using the dual Kantorovich formulation, we compute the strictly correlated electrons (SCE) functional (corresponding to the exact strong-interaction limit of density functional theory) for the hydrogen molecule along the dissociation curve. We use an exact relation between the Kantorovich potential and the optimal map to compute the comotion function, exploring corrections based on it. In particular, we analyze how the SCE functional transforms in an exact way the electron–electron distance into a one-body quantity, a feature that can be exploited to build new approximate functionals. We also show that the dual Kantorovich formulation provides in a natural way the constant in the Kohn–Sham potential recently introduced by Levy and Zahariev [*Phys. Rev. Lett.* **2014**, *113*, 113002] for finite systems.



## 1. INTRODUCTION

A good accuracy–price ratio makes Kohn–Sham Density Functional Theory (KS DFT)<sup>1</sup> the most used method for electronic structure calculations in various fields from biochemistry to material science. Unlike standard mean-field theories, KS DFT is, in principle, an exact theory: if the exchange–correlation functional  $E_{xc}[\rho]$  were known, KS DFT would yield the exact ground state energy and density of any many-electron system. In practice, different approximations for  $E_{xc}[\rho]$  are often used to tackle different classes of systems, properties, or processes, and despite enormous successes, there are still problems that hamper KS DFT’s overall predictive power. The lack of accuracy of KS DFT for certain systems is a reflection of the fundamental issues that present approximations still encounter.<sup>2,3</sup> In particular, the most challenging problems are related to near-degeneracy and strong correlation effects, where KS DFT easily gives even qualitatively wrong results. Crucial examples for chemistry are stretched bonds and systems containing d and f elements. In such cases, broken symmetry solutions often give better energies, but in complex systems they might be sensitive to the functional chosen, and they give a wrong characterization of several properties.<sup>4</sup>

Mainstream strategies to improve the approximations for the xc functional of KS theory follow the idea of a “Jacob’s ladder,”<sup>3,5</sup> based on an ansatz for the dependence of the xc functional on the relevant “ingredients,” increasing the complexity of the approximations in a hierarchical manner (local density, local density gradients, local KS kinetic energy, KS occupied orbitals, up to the KS virtuals). A (sometimes very large) number of parameters can be also introduced and fitted to specific data sets.<sup>6</sup> We have to keep in mind that KS DFT is based on a system of noninteracting Fermions, treating the electron–electron interactions in an approximate way. Current

available approximations mainly work when the physics of the true, interacting system is not too different from the noninteracting one of Kohn and Sham: for these cases, the “Jacob’s ladder” strategy proved to be highly successful in capturing the (relatively small) xc effects. Strongly correlated systems, however, are radically different from noninteracting ones. In these cases, the xc functional needs to be a drastic correction, and traditional strategies might not be the best path to follow.

A possible, rigorous starting point to build this drastic correction is provided by the limit of infinite coupling strength of the exact xc functional, called the “strictly-correlated electrons” (SCE) functional.<sup>7–9</sup> The SCE functional has a highly nonlocal dependence on the density that encodes new information with respect to the traditional ingredients of the “Jacob’s ladder” approach. Despite this high nonlocality, the SCE functional derivative with respect to the electronic density can be computed exactly via a powerful shortcut,<sup>10,11</sup> yielding a one-body multiplicative Kohn–Sham potential that is truly able to make noninteracting electrons reproduce key features of strongly correlated ones, without artificially breaking any symmetry, as shown by self-consistent KS SCE results on model semiconductor quantum wires and quantum dots.<sup>11,12</sup> The SCE functional has been also extended to fractional electron numbers,<sup>13</sup> displaying a derivative discontinuity at integer electron numbers in low-density systems even in a spin-restricted framework, a key property to describe the ground state of strongly correlated systems,<sup>2</sup> as well as important applications such as quantum transport,<sup>14</sup> missed by the standard approximate xc functionals.<sup>2</sup> Simple tests on one-

Received: April 24, 2015

Published: June 11, 2015

dimensional model chemical systems showed that the xc SCE functional is able to correctly stretch a bond in KS theory without symmetry breaking, while largely overcorrelating at weak- and intermediate correlation regimes. A very recent<sup>15</sup> numerical study on the three-dimensional H<sub>2</sub> molecule also found results that are in qualitative agreement with the one-dimensional ones, confirming that the latter were good models for the chemistry in this case, as inferred in ref 16. The challenge is then to retain the good performances of the SCE functional at strong correlation while adding corrections for (or interpolating to) the weak and intermediate chemically relevant correlation regimes. First corrections to KS SCE tested on one-dimensional models<sup>17</sup> and to the anions of the He isoelectronic series<sup>18</sup> have been found to improve substantially at different correlation regimes but are still not satisfactory.

Overall, the asymptotic exactness of the nonlocal physics of the xc SCE functional makes it a very promising ingredient to overcome the present problems of KS DFT, even if the SCE nonlocality is probably too extreme, and one will need to reduce it in some approximate way: a first step in this sense has been undertaken in ref 19. The original formulation of the SCE functional was based on the idea that, in the strong-interaction limit, the electrons are infinitely (or perfectly) correlated. A change of the position of one electron in the system affects the positions of all the others, a feature that is captured by mathematical objects, known as *comotion functions*  $\mathbf{f}_i(\mathbf{r})$ , which are nonlocal functionals of the density.<sup>7,8</sup> Alongside this original formulation, more recently another SCE formulation appeared, based on the mass transportation theory (or optimal transport) formalism,<sup>20–23</sup> an important field of mathematics and economics.<sup>24–26</sup> The optimal transport formulation defines a dual problem that corresponds to a maximization under linear constraints, yielding in one shot the functional and its functional derivative. First proof-of-principle calculations with this dual formulation have been carried out by Mendl and Lin.<sup>22</sup> To show that their algorithm works for a general 3D geometry, they have applied it to a model density for a trimer with up to six electrons, consisting of three different Gaussians centered arbitrarily, thus obtaining the SCE functional and potential bypassing the comotion functions. However, the dual formulation is expensive, as it involves a high-dimensional minimization. The formulation with the comotion functions is certainly more appealing (as it defines a sparse problem) and more physically transparent. A promising route to use the physics of the xc SCE functional to improve DFT approximations could be the construction of *approximate* comotion functions, i.e., to build functionals totally inspired to the SCE form, and to combine them with suitable corrections, like the ones of refs 17 and 18. To be able to approximate the comotion functions in general 3D geometry, it is essential to gain insight into their exact form as much as possible, as well as to understand if corrections based on them could really improve the KS SCE results.

In this work, we construct accurate comotion functions for the 3D hydrogen molecule along the dissociation curve, by means of a powerful result from mass transportation theory: for the special case of  $N = 2$  particles, it is possible from the dual formulation to obtain the comotion function in closed form (according to the basis chosen for the potential). Thus, we first implement the dual formulation using a physically motivated parametrization for the SCE potential (different from the one used by Mendl and Lin<sup>22</sup>), and we then extract the comotion function at different internuclear separations. We then compute

the full dissociation energy curve by using the bare xc SCE functional and by adding to it two corrections constructed using our accurate comotion function. As already observed in the 1D calculations and in ref 15, we find that the xc SCE functional is able to correctly dissociate the molecule in the spin-restricted KS formalism, but as expected, it gives total energies way too low near the equilibrium distance. Notice that in ref 15 the comotion function was obtained numerically, using a smart grid. Here we use a basis set approach, which is crucial to constructing corrections based on the comotion function itself. We find that using the comotion functions to build corrections largely improves the KS SCE results, providing dissociation curves significantly better than the ones from standard functionals. The interesting point is that the comotion function transforms rigorously a two-body property (the electron–electron distance) into a one-body quantity. We also show that the dual Kantorovich formulation provides in a natural way the Levy and Zahariev constant of the Kohn–Sham potential for finite systems<sup>27</sup> and that this constant has a very well-defined physical meaning in the strong-interaction limit of the DFT adiabatic connection.

## 2. KOHN–SHAM DFT WITH THE SCE FUNCTIONAL

The strictly correlated electrons (SCE) functional can be briefly introduced starting from the standard adiabatic connection in DFT, in which the electron–electron repulsion operator  $\hat{V}_{ee}$  in the Hohenberg–Kohn functional is rescaled by a real parameter  $\lambda$ :<sup>28,29</sup>

$$E_\lambda[\rho] = \min_{\Psi \rightarrow \rho} \langle \Psi | \hat{T} + \lambda \hat{V}_{ee} | \Psi \rangle \quad (1)$$

where, as usual,<sup>30</sup> the search is over all Fermionic wave functions  $\Psi$  yielding the density  $\rho(\mathbf{r})$ . The adiabatic connection provides an exact formula for the Hartree-exchange-correlation functional  $E_{\text{Hxc}}[\rho]$ :<sup>28,29</sup>

$$E_{\text{Hxc}}[\rho] = \int_0^1 \langle \Psi_\lambda[\rho] | \hat{V}_{ee} | \Psi_\lambda[\rho] \rangle d\lambda \equiv \int_0^1 V_{ee}^\lambda[\rho] d\lambda \quad (2)$$

where  $\Psi_\lambda[\rho]$  is the minimizing wave function in eq 1. Although  $\lambda$  in this formula varies only between 0 (the Kohn–Sham system) and 1 (the physical system), the situation in which  $\lambda > 1$  can provide very useful information to build approximations. The SCE functional  $V_{ee}^{\text{SCE}}[\rho]$  corresponds to the limit of infinite coupling strength,  $\lambda \rightarrow \infty$ , of the integrand in eq 2:

$$V_{ee}^{\text{SCE}}[\rho] = \lim_{\lambda \rightarrow \infty} V_{ee}^\lambda[\rho] = \langle \Psi_\infty[\rho] | \hat{V}_{ee} | \Psi_\infty[\rho] \rangle \quad (3)$$

and it is the natural counterpart of the KS noninteracting kinetic energy functional  $T_s[\rho] = F_{\lambda=0}[\rho]$ .

The SCE functional  $V_{ee}^{\text{SCE}}[\rho]$  was first introduced by Seidl and co-workers,<sup>7,8,31</sup> and it corresponds to the minimal Coulomb repulsion among all the wave functions that are consistent with  $\rho(\mathbf{r})$ . The square of the minimizing wave function,  $|\Psi_\infty[\rho]|^2$ , becomes a distribution in this limit,<sup>32</sup> and it describes the maximum possible correlation in the given density  $\rho(\mathbf{r})$ : if one of the electrons changes its position, the other electrons in the system would also change their positions, in such a way that the new interparticle distances continue to minimize the total Coulomb repulsion. If we label the position of one of the electrons in the  $N$ -electron system as  $\mathbf{r}$ , then  $\mathbf{r}$  would fix the position of all the other  $N - 1$  electrons via the so-called comotion functions  $\mathbf{f}_i(\mathbf{r})$ ,  $\mathbf{r}_i = \mathbf{f}_i(\mathbf{r})$ .<sup>8</sup> The comotion functions are nonlocal functionals of the one-electron density

$\rho(\mathbf{r})$ : the probability of finding the reference electron at position  $\mathbf{r}$  must be the same as the probability of finding the  $i$ th electron at  $\mathbf{f}_i(\mathbf{r})$ , a condition given via the following differential equations<sup>8</sup>

$$\rho(\mathbf{f}_i(\mathbf{r})) d\mathbf{f}_i(\mathbf{r}) = \rho(\mathbf{r}) d\mathbf{r} \quad (4)$$

As electrons are indistinguishable, the reference electron at  $\mathbf{r}$  could be any electron in the system, so the comotion functions need to satisfy the following cyclic group properties:<sup>8,9</sup>

$$\begin{aligned} \mathbf{f}_1(\mathbf{r}) &\equiv \mathbf{r}, \\ \mathbf{f}_2(\mathbf{r}) &\equiv \mathbf{f}(\mathbf{r}), \\ \mathbf{f}_3(\mathbf{r}) &= \mathbf{f}(\mathbf{f}(\mathbf{r})), \\ \mathbf{f}_4(\mathbf{r}) &= \mathbf{f}(\mathbf{f}(\mathbf{f}(\mathbf{r}))), \\ &\vdots \\ \underbrace{\mathbf{f}(\mathbf{f}(\dots \mathbf{f}(\mathbf{f}(\mathbf{r}))))}_{N \text{ times}} &= \mathbf{r} \end{aligned} \quad (5)$$

In terms of the comotion functions, the SCE functional  $V_{ee}^{\text{SCE}}[\rho]$  can be expressed as<sup>32</sup>

$$V_{ee}^{\text{SCE}}[\rho] = \frac{1}{2} \int d\mathbf{r} \rho(\mathbf{r}) \sum_{i=2}^N \frac{1}{|\mathbf{r} - \mathbf{f}_i(\mathbf{r})|} \quad (6)$$

Despite the high nonlocal character of the SCE functional, evident from eq 4, it is possible to find its exact functional derivative (yielding a one-body multiplicative potential) via the auxiliary equation<sup>10,11</sup>

$$\nabla v_{\text{SCE}}(\mathbf{r}) = - \sum_{i=2}^N \frac{\mathbf{r} - \mathbf{f}_i(\mathbf{r})}{|\mathbf{r} - \mathbf{f}_i(\mathbf{r})|^3} \quad (7)$$

which shows that the SCE potential  $v_{\text{SCE}}(\mathbf{r})$  exactly represents the net Coulomb repulsion acting on the electron at position  $\mathbf{r}$ , when the many-electron system is described by  $|\Psi_{\infty}[\rho]\rangle^2$ .

The SCE functional can be used to partition the Hohenberg–Kohn functional  $F[\rho] = F_{\lambda=1}[\rho]$  of eq 1 as

$$F[\rho] = T_s[\rho] + V_{ee}^{\text{SCE}}[\rho] + T_c[\rho] + V_{ee}^{\text{d}}[\rho] \quad (8)$$

where both the kinetic correlation energy,  $T_c[\rho] = \langle \Psi_{\lambda=1}[\rho] | \hat{T} | \Psi_{\lambda=1}[\rho] \rangle - T_s[\rho]$  and the electron–electron decorrelation energy<sup>33,34</sup>  $V_{ee}^{\text{d}}[\rho] = \langle \Psi_{\lambda=1}[\rho] | \hat{V}_{ee} | \Psi_{\lambda=1}[\rho] \rangle - V_{ee}^{\text{SCE}}[\rho]$  are positive.

If we neglect  $T_c[\rho]$  and  $V_{ee}^{\text{d}}[\rho]$ , we obtain the KS SCE approximation, which corresponds to set

$$E_{\text{Hxc}}[\rho] \approx V_{ee}^{\text{SCE}}[\rho] \quad (9)$$

and it is equivalent to approximate the minimum of the sum in the Hohenberg–Kohn functional with the sum of the two minima

$$\min_{\Psi \rightarrow \rho} \langle \Psi | \hat{T} + \hat{V}_{ee} | \Psi \rangle \approx \min_{\Psi \rightarrow \rho} \langle \Psi | \hat{T} | \Psi \rangle + \min_{\Psi \rightarrow \rho} \langle \Psi | \hat{V}_{ee} | \Psi \rangle \quad (10)$$

yielding a rigorous lower bound to the exact ground-state energy. Notice that in the low-density limit the sum of the Hartree and the exact xc functional tends asymptotically to the SCE functional.

### 3. THE SCE FUNCTIONAL AND MASS TRANSPORTATION THEORY

The link between the SCE functional and mass transportation (or optimal transport) theory was found, independently, by Buttazzo et al.<sup>20</sup> and by Cotar et al.<sup>21</sup> Mass transportation theory dates back to 1781 when Monge<sup>24</sup> posed the problem of finding the most economical way of moving soil from one area to another. In 1942, Kantorovich<sup>25</sup> generalized it to what is now known as the Kantorovich dual problem. In the past 20 years, optimal transport has developed into one of the most active fields in mathematics.<sup>26</sup> The basic Monge problem consists in asking what is the most economical way to move a mass distribution  $\rho_1(\mathbf{r})$  into another distribution  $\rho_2(\mathbf{r})$ , given the work  $c(\mathbf{r}_1, \mathbf{r}_2)$  (called *cost*) necessary to move a unit mass from a position  $\mathbf{r}_1$  to another position  $\mathbf{r}_2$ . The solution to the Monge problem is then given in terms of an *optimal map*, which assigns to every point  $\mathbf{r}$  of  $\rho_1(\mathbf{r})$  a unique final destination  $\mathbf{f}(\mathbf{r})$  in  $\rho_2(\mathbf{r})$ . The comotion functions turn out to be exactly the optimal maps for a multimarginal Monge problem with cost function given by the Coulomb repulsion.<sup>20</sup> However, it is very delicate to prove in general the existence of the set of optimal map functions for systems with arbitrary dimension and density (a formal proof for the SCE case is available, up to now, only for the one-dimensional case<sup>35</sup> with any number  $N$  of electrons, and for  $N = 2$  in any dimension and geometry<sup>20</sup>). It is for that reason that Kantorovich<sup>25</sup> proposed a relaxed formulation of the Monge problem, in which the goal is to find a *transport plan* that gives the probability that, at optimality, a given element  $\mathbf{r}_1$  of  $\rho_1$  be transported in  $\mathbf{r}_2$  in  $\rho_2$ . This relaxed problem, in turn, has a dual formulation, known as the dual Kantorovich problem, which is closely related to the Legendre transform formulation of standard DFT<sup>36</sup> and corresponds to a maximization with respect to potentials, under linear constraints. The maximizing Kantorovich potential  $u(\mathbf{r})$  differs from the SCE potential of eq 7  $v_{\text{SCE}}(\mathbf{r})$ —defined, for finite systems, as the functional derivative of  $V_{ee}^{\text{SCE}}[\rho]$  supplemented by the condition  $v_{\text{SCE}}(|\mathbf{r}| \rightarrow \infty) \rightarrow 0$ —only by a constant  $C[\rho]$ :<sup>20</sup>

$$u(\mathbf{r}) = v_{\text{SCE}}(\mathbf{r}) + C[\rho] \quad (11)$$

As we shall discuss more in detail in section 7, the constant  $C[\rho]$  appearing in the Kantorovich potential is exactly the same (in the strong-correlation limit) as that recently introduced by Levy and Zahariev.<sup>27</sup>

From the optimal-transport point of view, the SCE functional defines a multimarginal problem, in which all the marginals are the same, so that the SCE mass-transportation problem corresponds to a reorganization of the “mass pieces” within the same density. The dual Kantorovich formulation for  $V_{ee}^{\text{SCE}}[\rho]$ , defining the Kantorovich potential  $u(\mathbf{r})$ , is<sup>20</sup>

$$\begin{aligned} V_{ee}^{\text{SCE}}[\rho] &= \max_u \left\{ \int u(\mathbf{r}) \rho(\mathbf{r}) d\mathbf{r} : \sum_{i=1}^N u(\mathbf{r}_i) \right. \\ &\leq \left. \sum_{i=1}^N \sum_{j>i}^N \frac{1}{|\mathbf{r}_i - \mathbf{r}_j|} \right\} \end{aligned} \quad (12)$$

Equation 12 is a linear programming problem with an infinite number of constraints, which could be dealt with by readapting optimal transport algorithms to the SCE functional, a research goal that is the object of ongoing efforts.<sup>37,38</sup> In a brute force approach, Mendl and Lin<sup>22</sup> reformulated the problem in terms



of a nested optimization, by introducing a functional  $g[v_{\text{SCE}}]$  of  $v_{\text{SCE}}(\mathbf{r})$ :

$$g[v_{\text{SCE}}] = \min_{\{\mathbf{r}_i\}} \sum_{i=1}^N \sum_{j>i}^N \frac{1}{|\mathbf{r}_i - \mathbf{r}_j|} - \sum_{i=1}^N v_{\text{SCE}}(\mathbf{r}_i) \quad (13)$$

and then showed that  $V_{\text{ee}}^{\text{SCE}}[\rho]$  can be found via the following nested optimization:

$$\begin{aligned} V_{\text{ee}}^{\text{SCE}}[\rho] &= \max_{v_{\text{SCE}}} \left\{ \int v_{\text{SCE}}(\mathbf{r}) \rho(\mathbf{r}) \, \text{d}\mathbf{r} + g[v_{\text{SCE}}] \right\} \\ &= \max_{v_{\text{SCE}}} \left\{ \min_{\{\mathbf{r}_i\}} \left\{ \sum_{i=1}^N \sum_{j>i}^N \frac{1}{|\mathbf{r}_i - \mathbf{r}_j|} - \sum_{i=1}^N v_{\text{SCE}}(\mathbf{r}_i) \right\} \right. \\ &\quad \left. + \int v_{\text{SCE}}(\mathbf{r}) \rho(\mathbf{r}) \, \text{d}\mathbf{r} \right\} \quad (14) \end{aligned}$$

Equation 14 is equivalent to eq 12 of ref 8, obtained by generalizing the Lieb Legendre transform formulation<sup>36</sup> to the SCE functional.

Notice that eq 12 defines a particular gauge for the Kantorovich potential  $u(\mathbf{r})$ , since a constant could be added to the left-hand side of the inequality yielding a shifted potential. The Kantorovich potential is historically defined in such a way that  $\int \rho(\mathbf{r}) u(\mathbf{r}) \, \text{d}\mathbf{r}$  gives exactly the optimal cost.

## 4. THE SCE FUNCTIONAL FOR THE HYDROGEN MOLECULE

**4.1. Kantorovich Formulation.** To solve the Kantorovich problem for the  $\text{H}_2$  molecule, we have used cylindrical coordinates  $(z, h, \theta)$ . The two protons lie along the  $z$  axis, with the molecular center of inversion at the origin of the coordinate system.  $h$  denotes the distance from the  $z$  axis, and  $\theta$  is the azimuthal angle. Since the electron density does not depend on  $\theta$ ,  $\rho(\mathbf{r}) = \rho(h, z)$ , we have  $v_{\text{SCE}}(\mathbf{r}) = v_{\text{SCE}}(h, z)$ . Minimization of the SCE classical potential energy<sup>8</sup> immediately yields for the azimuthal angles of the two electrons  $|\theta_1 - \theta_2| = \pi$  for any values of the other four coordinates, resulting in a four-dimensional potential energy function:

$$\begin{aligned} E_{\text{pot}} &= -v_{\text{SCE}}(z_1, h_1) - v_{\text{SCE}}(z_2, h_2) \\ &\quad + \frac{1}{\sqrt{(h_1 + h_2)^2 + (z_1 - z_2)^2}} \quad (15) \end{aligned}$$

In order to parametrize the SCE potential  $v_{\text{SCE}}(\mathbf{r})$ , Mendl and Lin<sup>22</sup> introduced a “pseudocharge”  $m(\mathbf{r})$  to solve eq 14 numerically:

$$v_{\text{SCE}}(\mathbf{r}) = \int \frac{m(\mathbf{r}')}{|\mathbf{r} - \mathbf{r}'|} \, \text{d}\mathbf{r}' \quad (16)$$

with the following constraint on it:

$$\int m(\mathbf{r}) \, \text{d}\mathbf{r} = N - 1 \quad (17)$$

The role of the “pseudocharge” is to preserve the asymptotic behavior of the SCE potential. Being a functional derivative of a self-interaction free functional, the SCE potential decays for  $|\mathbf{r}| \rightarrow \infty$  as  $(N - 1)/|\mathbf{r}|$ .<sup>8,10,11</sup> They solved the Kantorovich dual problem for small atoms and a model trimer molecule (with up to six electrons) parametrizing the “pseudocharges” with

gaussians centered along the three axes joining the three “atoms” with the symmetry center of the “molecule.”

Here, we want to include the physics behind the SCE problem in the parametrization of  $v_{\text{SCE}}(\mathbf{r})$ . From eq 7, we see that SCE transforms the electron–electron repulsion into an effective one-body potential that exerts the same net force. This potential has, on the density of noninteracting electrons, the same effects of the electron–electron repulsion: it increases charge localization on the atoms, reducing charge in the midbond region.<sup>39</sup> This is realized through “bumps” or barriers in the potential. The bumps are present in the exact  $v_{\text{Hxc}}(\mathbf{r})$  and  $v_{\text{SCE}}(\mathbf{r})$ , and they are crucial to capturing the physics of charge localization in strongly correlated systems within the KS framework.<sup>11,12,39,40</sup> The standard approximate KS potentials lack this feature, displaying the well-known deficiencies of approximate DFT.<sup>41</sup> The bump is present at the bond midpoint of  $\text{H}_2$  at longer internuclear distances, and it localizes the electrons around the protons.<sup>39,40</sup> If one uses the “pseudocharge” algorithm of Mendl and Lin with the pseudocharges centered between the center of the molecule and the two H atoms, the corresponding  $v_{\text{SCE}}(\mathbf{r})$  will have two bumps, instead of one at the bond midpoint.

In this work, we parametrize  $v_{\text{SCE}}(\mathbf{r})$  directly, by modeling the bump in the midbond region. Taking into account the asymptotic behavior of the SCE potential and the symmetry of the  $\text{H}_2$  molecule, we use the following ansatz for  $v_{\text{SCE}}(\mathbf{r})$ :

$$v_{\text{SCE}}(z, h) = \sum_{i=1}^m A_i e^{-p_i z^2 - q_i h^2} + \frac{\text{erf}(a\sqrt{h^2 + z^2})}{\sqrt{h^2 + z^2}} \quad (18)$$

where  $A_i$ ,  $p_i$ ,  $q_i$ , and  $a$  are a set of parameters. The SCE potential of eq 18 decays as  $1/|\mathbf{r}|$  for large  $\mathbf{r}$ , and the ansatz is flexible enough to create a bump around the bond midpoint. In particular, the sum of gaussians models the part of the potential around the midbond, being able to capture the features analyzed in refs 40 and 39, while the second term in the right-hand side of eq 18 ensures the correct long-range decay.

We have performed the nested optimization of eq 14 to calculate  $V_{\text{ee}}^{\text{SCE}}[\rho]$  on a postfunctional level from a FCI density obtained from the GAMESS-US package,<sup>42</sup> within the aug-cc-pV6Z basis set of Dunning.<sup>43</sup> We fitted the obtained density on a sum of Gaussian functions centered along the nuclear axis, so the density reads as follows:

$$\rho(z, h) = \sum_{i=1}^Q \alpha_i (e^{-\beta_i^2((z-\gamma_i)^2+h^2)} + e^{-\beta_i^2((z+\gamma_i)^2+h^2)}) \quad (19)$$

where  $\alpha_i$ ,  $\beta_i$ , and  $\gamma_i$  are fitting parameters. This way, the term  $\int v_{\text{SCE}}(\mathbf{r}) \rho(\mathbf{r}) \, \text{d}\mathbf{r}$  which appears in eq 14 can be evaluated analytically (see Appendix). The nested optimization of eq 14 has then been done numerically for a set of interatomic distances.

**4.2. Dissociation Curve from the Kantorovich Problem.** From the numerical maximization of eq 14, we have obtained  $V_{\text{ee}}^{\text{SCE}}[\rho]$ . From the same density, we also constructed  $T_s[\rho]$  and the expectation of the external potential. The resulting KS SCE dissociation curve is shown in Figure 1. We compare the KS SCE results with those of the B3LYP functional, restricted Hartree–Fock (HF), full-CI, and the nonlocal radius functional (NLR),<sup>19</sup> which is meant to be an approximation for KS SCE. The B3LYP, restricted HF and full-CI dissociation curves were calculated with the GAMESS-US package,<sup>42</sup> within the same aug-cc-pV6Z basis set of Dunning.<sup>43</sup>

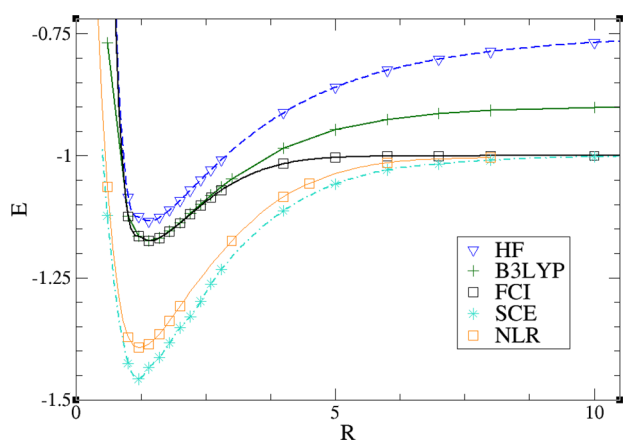


**Figure 1.**  $H_2$  dissociation curve obtained by the following methods: restricted Hartree–Fock, B3LYP, FCI, KS SCE, and NLR functional of ref 19, an approximation of the KS SCE method.

The NLR functional is built from a model for the xc hole in the strong-correlation limit, whose details are given in ref 19, and the NLR data in Figure 1 were taken from the same reference.

As expected from the 1D model studied in ref 17 and the 3D implementation of ref 15, we see that around equilibrium the KS SCE error is very large, due to the tendency of KS SCE to overcorrelate the electrons. With the increase of the internuclear distance, KS SCE starts to be more accurate, becoming exact in the dissociation limit. The accuracy of the KS SCE functional in the limit  $R \rightarrow \infty$  can be understood by

looking at the shape of the very accurate adiabatic connection curves  $W_\lambda[\rho] = V_{\text{ec}}^\lambda[\rho] - E_{\text{H}}[\rho]$  for  $H_2$  obtained by Teale et al.<sup>44</sup> The slope of  $W_\lambda[\rho]$  at  $\lambda = 0$  is getting more negative as the bond length increases, and it diverges at the dissociation limit. For shorter bond lengths, the exact  $W_\lambda[\rho]$  curve for  $0 \leq \lambda \leq 1$  is significantly above the  $W_\infty[\rho]$  value ( $W_\lambda[\rho] \approx W_\infty[\rho]$  corresponds to the KS SCE approximation). This leads to a serious overestimation (in absolute terms) of the (negative) area above the  $W_\lambda[\rho] = W_\infty[\rho]$  line with respect to the area above the exact  $W_\lambda[\rho]$  curve. On the other hand, for large bond lengths, the accurate adiabatic curves have a very negative slope at  $\lambda = 0$  with  $W_\lambda[\rho]$  values close to  $W_\infty[\rho]$ , even for small positive values of  $\lambda$ . This results in a very small difference between  $W_\infty[\rho]$  and  $E_{\text{xc}}[\rho]$  for large finite bond lengths, the two becoming equal as the separation between the two protons goes to infinity.

The NLR functional<sup>19</sup> results are very close to the ones from the KS SCE functional, showing that the former is a good approximation for the latter.

The bond length from KS SCE is also significantly shorter ( $\sim 1.2$  au) than the exact one ( $\sim 1.4$  au). This is due to the fact that, as we stretch the bond, the nuclear–electron expectation value increases, while the electron–electron and nuclear–nuclear repulsions decrease. The KS SCE method seriously underestimates the electron–electron repulsion in the equilibrium region (as the electrons perfectly avoid each other, they can have a very low electron–electron repulsion expectation even in a compact density), while the other components (including  $T_s[\rho]$ ) are the same. Therefore, KS SCE lowers the

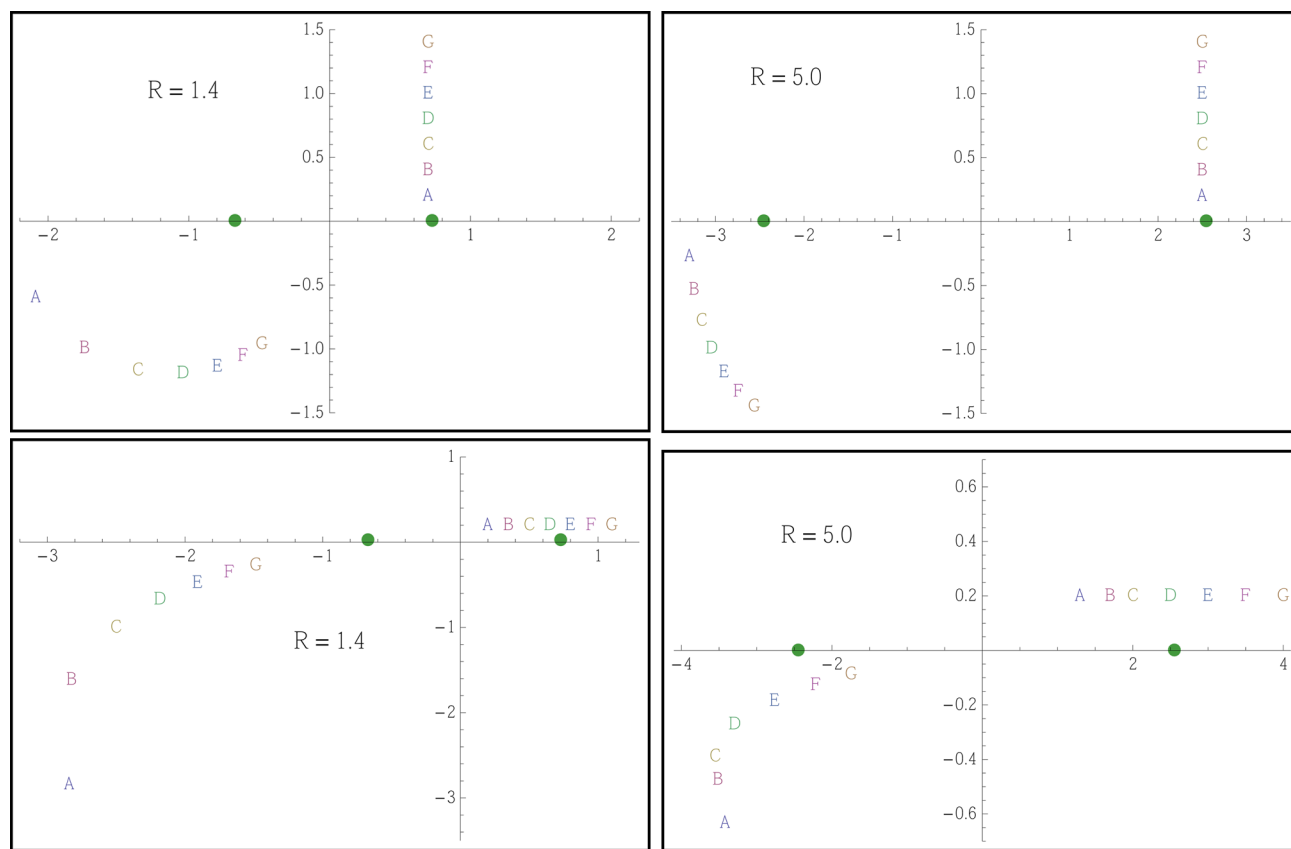


**Figure 2.** Samples of strictly correlated positions  $\{\mathbf{r}, f(\mathbf{r})\}$  for the  $H_2$  molecule at equilibrium ( $R = 1.4$ ) and in a stretched configuration ( $R = 5.0$ ). The two nuclei in each case lie along the horizontal axis and are shown with green filled circles. Each pair of strictly correlated positions is labeled with the same letter, e.g.,  $\{A, A\} = \{\mathbf{r}_A, f(\mathbf{r}_A)\}$ .

price that has to be paid to shorten the bond length. The KS SCE method also misses  $T_c[\rho]$ , but the error from this absence is significantly smaller than the error for the electronic repulsion.

**4.3. Comotion Function from the Kantorovich Problem.** Once we have solved the Kantorovich problem, we already have the value of  $V_{ee}^{SCE}[\rho]$  (the maximum in eq 14), and its functional derivative (the maximizing potential in eq 14), so that we can bypass the comotion functions. However, as said, the comotion functions can be used to build corrections beyond KS SCE (which are the object of the next section 5) and to build approximations to the SCE functional.

In the special case  $N = 2$ , we can obtain the comotion function  $\mathbf{f}(\mathbf{r})$  from the Kantorovich potential<sup>20</sup> by solving eq 7 for  $\mathbf{f}(\mathbf{r})$ :

$$\mathbf{f}(\mathbf{r}) = \mathbf{r} + \frac{\nabla v_{SCE}(\mathbf{r})}{|\nabla v_{SCE}(\mathbf{r})|^{3/2}} \quad (20)$$

which, in our case, corresponds to obtaining the  $f_z$  and  $f_h$  components of the comotion function in cylindrical coordinates:

$$f_z(z, h) = z + \frac{\frac{\partial v_{SCE}(z, h)}{\partial z}}{\left( \left( \frac{\partial v_{SCE}(z, h)}{\partial z} \right)^2 + \left( \frac{\partial v_{SCE}(z, h)}{\partial h} \right)^2 \right)^{3/4}} \quad (21)$$

$$f_h(z, h) = \left| h + \frac{\frac{\partial v_{SCE}(z, h)}{\partial h}}{\left( \left( \frac{\partial v_{SCE}(z, h)}{\partial z} \right)^2 + \left( \frac{\partial v_{SCE}(z, h)}{\partial h} \right)^2 \right)^{3/4}} \right| \quad (22)$$

The computed comotion function satisfies the group properties in eq 5, which, in this case, is just  $\mathbf{f}(\mathbf{f}(\mathbf{r})) = \mathbf{r}$ . This can be easily verified by simply noticing that it always holds  $\nabla v_{SCE}(\mathbf{r}) = -\nabla v_{SCE}(\mathbf{f}(\mathbf{r}))$  (action-reaction principle).

In Figure 2, we show samples of strictly correlated positions  $\{\mathbf{r}, \mathbf{f}(\mathbf{r})\}$  for the  $H_2$  molecule density at equilibrium distance,  $R = 1.4$ , and at a stretched configuration,  $R = 5.0$ . The two nuclei lie on the horizontal axis and are denoted with green filled circles. We have selected a series of positions  $\mathbf{r}_A, \mathbf{r}_B, \dots$  by placing the reference electron close to the right nucleus and moving it away from it perpendicularly to the bond axis. We have also set the reference electron at a distance of 0.2 au from the bond axis, and we have moved it parallel to it. The corresponding positions  $\mathbf{f}(\mathbf{r}_A), \mathbf{f}(\mathbf{r}_B), \dots$  appear, as expected, below the left nucleus.

## 5. CORRECTIONS TO THE SCE FUNCTIONAL FOR THE $H_2$ MOLECULE

The KS SCE approximation is very accurate for systems that are close to the strongly correlated regime. However, as soon as the effect of correlation is not profound, the KS SCE energies are unacceptably low. While in some systems studied in physics, such as electrons confined at semiconductor heterostructure interfaces in quasi-1D<sup>11</sup> and quasi-2D geometries,<sup>12</sup> the amount of correlation is directly related to a single parameter, so that it is possible to predict when KS SCE will be accurate, chemical systems are more delicate in that sense: they are often in between the strong and the weak correlation regimes, and it is not easy to say *a priori* whether the system is very correlated or

not. It is for that reason that we need to have “indicators” that can signal whether the overcorrelation of the SCE functional needs to be suppressed.

To recover the Hohenberg–Kohn functional starting from KS SCE, we have to construct the functionals  $T_c[\rho]$  and  $V_{ee}^d[\rho]$  of eq 8. We consider here two different approaches to construct the correcting terms, both based on the use of the comotion function  $\mathbf{f}(\mathbf{r})$ .

**5.1. Corrections Based on the SCE Interparticle Distance.** In refs 11, 18, and 19, a simple correction to KS SCE in terms of the local density only (so without using the comotion functions) has been introduced. The correction was based on the idea of making the approximate Hohenberg–Kohn functional  $F[\rho] = T_s[\rho] + V_{ee}^{SCE}[\rho] + E_{kcd}[\rho]$  exact for the homogeneous electron gas (HEG), where  $E_{kcd}[\rho]$  is an approximation for  $T_c[\rho] + V_{ee}^d[\rho]$ . This requires adding in the exchange-correlation energy of the HEG (i.e., the LDA xc energy) and subtracting out the SCE xc energy evaluated on the uniform gas:  $E_{kcd}[\rho] \approx E_{xc}^{LDA}[\rho] - W_{\infty}^{LDA}[\rho]$ . The term  $W_{\infty}^{LDA}[\rho]$  was obtained by using the common assumption that the SCE ( $\lambda$  or  $r_s \rightarrow \infty$ ) xc energy of the HEG can be obtained from the energy of the bcc Wigner crystal. This assumption, however, has recently been questioned,<sup>45</sup> so that it is actually not known what is the exact value of the SCE xc energy of the HEG: we only know that it has the form  $-c/r_s$ , and we have some bounds for the positive constant  $c$ .<sup>45</sup> Disregarding for a moment this issue, we can, as in refs 11 and 18, evaluate the xc energy densities (for both LDA and SCE), as usual, in terms of the local Wigner–Seitz radius

$$r_s(\mathbf{r}) = \frac{1}{\left( \frac{4}{3}\pi\rho(\mathbf{r}) \right)^{1/3}} \quad (23)$$

Unfortunately, this approximation turns out to be very drastic. We have found that, for  $H_2$ , it yields energies that are even higher than the Hartree–Fock ones. Even worse, this approximation fails to recognize one-electron systems (such as H or  $He^+$ ) and effectively one-electron regions (such as those in stretched  $H_2$ ) as noninteracting, which is one of the strengths of the SCE method. This problem is independent of the value we use for the constant  $c$  in the SCE xc energy of the HEG: it stems from the local nature of the correction.

In the stretched  $H_2$  molecule, the local density on each proton is high, so that the LDA approximation is obviously physically wrong: it assigns to the xc energy the same value as for a high-density, weakly correlated HEG. The stretched  $H_2$  molecule is, physically, more similar to a Wigner crystal, where the electrons are kept apart due to the dominance of their mutual repulsion. In the HEG, the Wigner–Seitz radius  $r_s$  is a measure of the average electron–electron distance. The comotion function allows us to recognize, in each point of space, that the interelectronic distance is large, even when the local density is high. This can be done by redefining the Wigner–Seitz radius as the distance between the two electrons, which can be uniquely determined in the SCE framework at each point in space:

$$r_s^{SCE}(\mathbf{r}) = |\mathbf{r} - \mathbf{f}(\mathbf{r})| \quad (N = 2) \quad (24)$$

The  $r_s^{SCE}(\mathbf{r})$  radius encodes two-body property information on highly nonlocal character (in terms of the density), despite being a one-body property itself. This is crucial for systems such as stretched  $H_2$ , where the effective Wigner–Seitz radius should go like the increasingly large bond-length  $R$  in regions

near the atoms, but where the usual local Wigner-Seitz radius  $r_s(\mathbf{r})$  is on the order of 1. The standard local density functional radius  $r_s(\mathbf{r})$  thus produces a correction which is nonzero as  $R \rightarrow \infty$ , unlike the nonlocal density functional radius  $r_s^{\text{SCE}}(\mathbf{r})$ , which dissociates significantly better. A similar definition (retaining the nearest neighbor distance) would also work for a chain of H atoms, but for larger molecules one should think of a more general definition, in order to distinguish core and valence.

The simplest way to build approximations based on the radius  $r_s^{\text{SCE}}(\mathbf{r})$  is to insert it into the LDA correction used in refs 11 and 18, replacing the standard Wigner-Seitz  $r_s(\mathbf{r})$ . In Figure 3, we show the dissociation curve for  $\text{H}_2$  corresponding to this

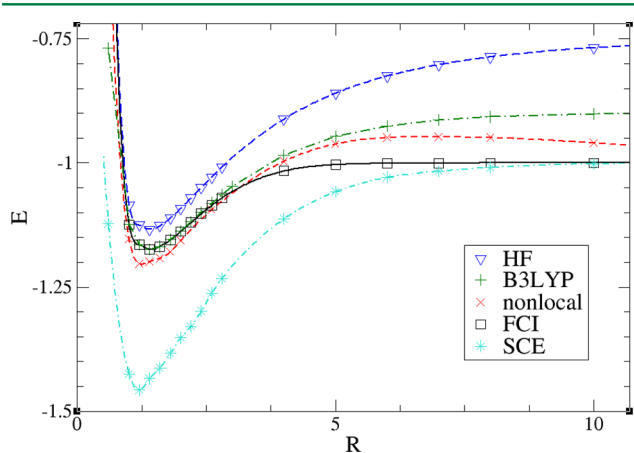


**Figure 3.**  $\text{H}_2$  dissociation curves obtained by the following methods: restricted Hartree–Fock, B3LYP, FCI, LDA correction with the redefined Wigner–Seitz radius of eq 24 added to KS SCE and KS SCE.

approximation (curve labeled “nonlocal”). The energies at the equilibrium region are substantially improved with the respect to KS SCE. However, although asymptotically the right dissociation limit is reached when  $R \rightarrow \infty$ , the limit is approached too slowly, producing a positive region in the dissociation curve, similarly to other methods such as the random-phase-approximations.<sup>46</sup> One of the biggest challenges for chemistry is, indeed, to bridge the weak and the strong correlation regimes in the right way.

In general, the two-body information encoded in  $r_s^{\text{SCE}}(\mathbf{r})$  can be used in many different ways to build approximate functionals. Other promising routes could be also based on the exploration of the kinetic correlation part (which is still very important also at strong correlation<sup>9,47</sup>), using the SCE conditional amplitude.<sup>40,48</sup>

**5.2. Restricted Mode Zero Point Energy Correction.** If we expand the Hohenberg–Kohn functional around  $\lambda \rightarrow \infty$ , the next leading term after the SCE functional should be given by zero-point oscillations around the SCE minimum,<sup>9</sup> although there is still no rigorous proof for that, but only numerical evidence.<sup>33,49</sup> The expansion of the integrand in eq 2 around  $\lambda \rightarrow \infty$  should be<sup>9</sup>

$$V_{\text{ee}}^{\lambda \rightarrow \infty}[\rho] = V_{\text{ee}}^{\text{SCE}}[\rho] + \frac{V_{\text{ee}}^{\text{ZPE}}[\rho]}{\sqrt{\lambda}} + O(\lambda^{-p}) \quad (25)$$

where  $p \geq 5/4$ , and the “ZPE” acronym stands for the “zero-point energy,” corresponding to the vibrational energy of small electronic oscillations around their SCE positions. For  $N$  electrons in  $D$  dimensions, this energy has the simple form<sup>9,17</sup>

$$V_{\text{ee}}^{\text{ZPE}}[\rho] = \frac{1}{2} \int d\mathbf{r} \frac{\rho(\mathbf{r})}{N} \sum_{n=1}^{DN-D} \frac{\omega_n(\mathbf{r})}{2} \quad (26)$$

The electron vibrational frequencies are defined as<sup>9</sup>

$$\omega_n(\mathbf{r}) = \sqrt{a_n(\mathbf{r})} \quad (27)$$

where  $a_n(\mathbf{r})$  are the eigenvalues of the Hessian matrix composed of the second order derivatives of the potential energy of the SCE system (eq 15 with the angular degrees of freedom included) with respect to all the electronic coordinates. Inserting the expansion of eq 25 into eq 2, we obtain the correction for  $T_c[\rho]$  and  $V_{\text{ee}}^{\text{d}}[\rho]$ :<sup>9,17</sup>

$$T_c[\rho] \approx V_{\text{ee}}^{\text{d}}[\rho] \approx V_{\text{ee}}^{\text{ZPE}}[\rho] \quad (28)$$

as expected from the fact that the ZPE is half kinetic and half potential energy. The total correction  $T_c[\rho] + V_{\text{ee}}^{\text{d}}[\rho]$  is generally too large.<sup>17</sup> However, one can argue that for chemical systems usually  $T_s[\rho]$  is much closer to the true kinetic energy than  $V_{\text{ee}}^{\text{SCE}}[\rho]$  to the true expectation of  $\hat{V}_{\text{ee}}$ , so that by correcting only the electron–electron part the balance is restored. In what follows, we then consider the correction  $T_c[\rho] \approx 0$ , and  $V_{\text{ee}}^{\text{d}}[\rho] \approx V_{\text{ee}}^{\text{ZPE}}[\rho]$ .

We also make another approximation, in order to simplify the calculations: we approximate the Hessian matrix with respect to the symmetry of the system, allowing the two electrons to vibrate only in a plane. The plane is determined by their two SCE positions and the internuclear axis. This approximation sets all the derivatives of  $E_{\text{pot}}$  with respect to the azimuthal coordinates ( $\theta_1$  and  $\theta_2$ ) to 0. We call this approximation restricted-mode zero-point oscillations (rm-ZPE).

In Figure 4, we show the dissociation energy curve with this correction. Again, we see that the energy is highly improved at

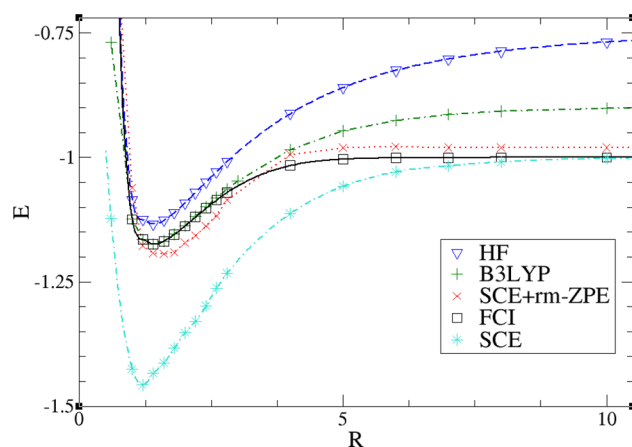


**Figure 4.**  $\text{H}_2$  dissociation curves obtained by the following methods: restricted Hartree–Fock, B3LYP, FCI, KS SCE with correction for the electron–electron energy obtained by the restricted-mode zero-point oscillations (rm-ZPE) of electrons and KS SCE.

equilibrium and that the exact dissociation limit is reached too slowly, even if better than with the nonlocal correction of the previous section.

## 6. ENERGY DENSITIES

Modeling the adiabatic connection has been an important milestone in the construction of approximate xc density



functionals (see, e.g., refs 50–53). While most approximations focus on the physically relevant regime  $0 \leq \lambda \leq 1$ , interpolating between the  $\lambda \rightarrow 0$  and  $\lambda \rightarrow \infty$  limits seems a rigorous way to overcome our lack of knowledge about the  $\lambda = 1$  region. The interaction strength interpolation (ISI) of Seidl and co-workers<sup>7,31</sup> is a pioneering density functional of this latter class. Newer interpolation models, such as the revised ISI<sup>9</sup> and the recent interpolation models of Liu and Burke,<sup>54</sup> have a functional form that behaves better than ISI about the  $\lambda \rightarrow \infty$  limit. These functionals are able to treat different correlation regimes accurately, but the development of DFT in this direction encounters a fundamental problem: the lack of size consistency, as these functionals depend nonlinearly on global (integrated over all space) quantities.

Size consistency in the usual DFT sense (see also refs 55 and 56, for a critical review) can be recovered if the interpolation is done locally along the adiabatic connection.<sup>32</sup> A local version of eq 2 for the xc energy is given by

$$E_{xc}[\rho] = \int d\mathbf{r} \rho(\mathbf{r}) \int_0^1 d\lambda w_\lambda[\rho](\mathbf{r}) \quad (29)$$

It is important to note that a choice of  $w_\lambda(\mathbf{r})$  is not unique, as we can add to it any quantity that integrates to zero when multiplied by  $\rho(\mathbf{r})$  and still get the same  $E_{xc}[\rho]$ . For this reason, it is very important to do the interpolation within the same definition or the same “gauge” of the energy density for all the ingredients used (e.g., at  $\lambda = 0$  and  $\lambda = \infty$ ). A physically sound and commonly used “gauge” of the energy density is the one given in terms of the xc hole potential:<sup>32,57,58</sup>

$$w_\lambda[\rho](\mathbf{r}) = \frac{1}{2} \int \frac{h_{xc}^\lambda(\mathbf{r}, \mathbf{r}')}{|\mathbf{r} - \mathbf{r}'|} d\mathbf{r}' \quad (30)$$

where  $h_{xc}^\lambda(\mathbf{r}, \mathbf{r}')$  is the xc hole obtained from the wave function  $\Psi_\lambda[\rho]$  of eq 2.

At  $\lambda = 0$ , this energy density corresponds to the usual exchange-hole potential,  $w_0(\mathbf{r}) = \epsilon_x(\mathbf{r})$ , while for  $\lambda \rightarrow \infty$  we have<sup>32</sup>

$$w_\infty(\mathbf{r}) = \frac{1}{2} \sum_{i=2}^N \frac{1}{|\mathbf{r} - \mathbf{f}_i(\mathbf{r})|} - \frac{1}{2} v_H(\mathbf{r}) \quad (31)$$

where  $v_H(\mathbf{r})$  is the Hartree potential. Notice that the SCE formalism yields, correctly, an energy density that decays at infinity like  $-(1/(2|r|))$  (in the gauge of the xc hole potential), and a functional derivative (xc potential) with the correct decay  $-(1/|r|)$ .

In Figure 5, we show the SCE energy density  $w_\infty(\mathbf{r})$  in the “gauge” of eq 30 at  $R = 1.4$  and  $R = 8.0$  along the internuclear axis ( $\hat{h} = 0$ ), together with the  $w_0(\mathbf{r})$  and  $w_1(\mathbf{r})$  curves. The SCE energy density  $w_\infty(\mathbf{r})$  of eq 31 has been calculated from the comotion function described in section 4.3, while  $w_0(\mathbf{r})$  and  $w_1(\mathbf{r})$  were taken from ref 32. All three quantities  $w_0(\mathbf{r})$ ,  $w_1(\mathbf{r})$ , and  $w_\infty(\mathbf{r})$  correspond to the full-CI density obtained from the GAMESS-US package,<sup>42</sup> within the aug-cc-pVTZ basis set of Dunning.<sup>43</sup> As expected, near the equilibrium ( $R = 1.4$ ) the physical energy is much closer to  $w_0(\mathbf{r})$  than  $w_\infty(\mathbf{r})$ . On the other hand, for the stretched ( $R = 8.0$ ) molecule, the physical energy density is much closer to  $w_\infty(\mathbf{r})$ . For this reason, the inclusion of the exact  $w_\infty[\rho](\mathbf{r})$  (or of a good model for it<sup>19,32</sup>) as an ingredient to build local interpolations along the adiabatic connection is a very promising approach for the treatment of strong correlation in DFT.

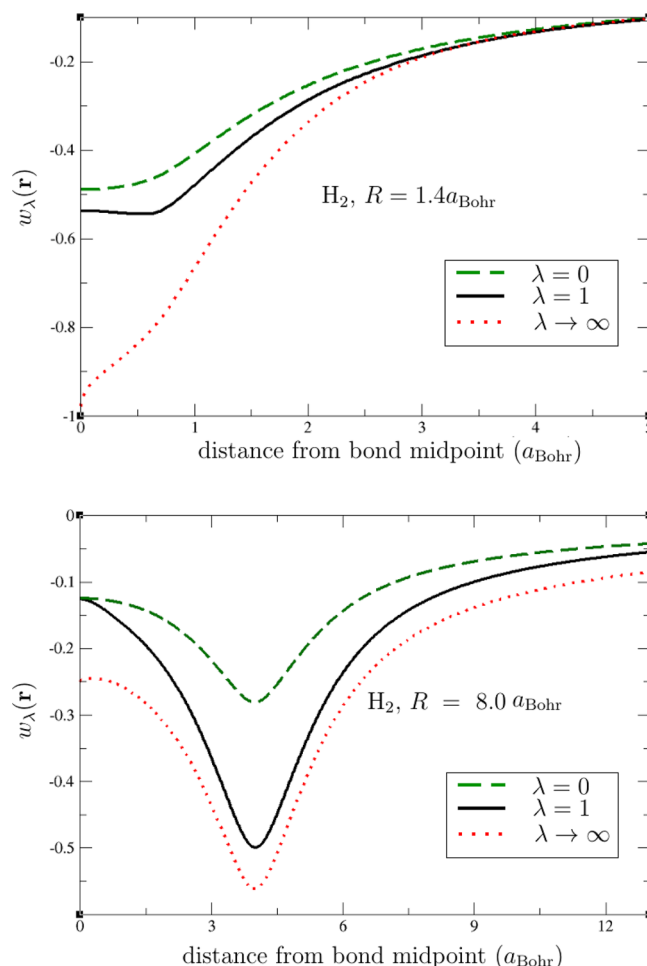


**Figure 5.** Energy densities in the gauge of the xc hole of eq 30 for  $H_2$  at  $R = 1.40$  and  $R = 8.0$  at different  $\lambda$  values: 0, 1, and  $\infty$ .

From Figure 5 we see that the SCE energy density displays a cusp at the bond midpoint. This is a feature related to the fact that when  $|r| \rightarrow 0$  the comotion function goes to infinity. Depending on how fast  $|f(\mathbf{r})|$  tends to infinity, the cusp might arise or not. Similarly, a cusp might or might not appear also in the SCE potential  $v_{SCE}(\mathbf{r})$  at the origin. The ansatz of eq 18 can capture a cusp in the potential with a very peaked Gaussian, similarly to how Gaussian basis sets fit the nuclear cusp of a Slater orbital.

## 7. THE CONSTANT OF LEVY AND ZAHARIEV IN THE STRONG-INTERACTION LIMIT OF DFT

For finite systems in chemistry, one usually defines the arbitrary constant that appears in the Hamiltonian by making the external potential go to zero as the distance from the center of nuclear charge goes to infinity. When turning to the KS system, this choice defines unequivocally the Hartree exchange-correlation energy  $E_{Hxc}[\rho]$ , whose functional derivative within the set of number conserving densities is, in turn, defined modulo a constant (see refs 59 and 60, for a complete discussion). Usually, the constant in the functional derivative is also chosen such that the Hartree-exchange-correlation potential goes to zero at large distances from the center of charge.

It has often been argued that it is easier to model the xc potential rather than the xc functional, since more is known



about the exact properties of the former.<sup>61,62</sup> In general, however, a given approximation for the xc potential is not necessarily a functional derivative, which means that the xc energy corresponding to it is not well-defined, although different solutions have been proposed.<sup>61,62</sup> Levy and Zahariev<sup>27</sup> showed that the physical ground state energy becomes equal to the sum of the occupied KS orbital energies if the corresponding Hxc potential is shifted by a nontrivial constant  $C[\rho]$  (with respect to the usual choice mentioned above) equal to

$$C[\rho] = \frac{E_{\text{Hxc}}[\rho] - \int v_{\text{Hxc}}[\rho](\mathbf{r}) \rho(\mathbf{r}) \, d\mathbf{r}}{\int \rho(\mathbf{r}) \, d\mathbf{r}} \quad (32)$$

They suggested that it might be easier to model the shifted potential  $\bar{v}_{\text{Hxc}}[\rho](\mathbf{r}) \equiv v_{\text{Hxc}}[\rho](\mathbf{r}) + C[\rho]$  rather than the usual xc potential that goes to zero asymptotically. Although in general the model potential would not be a functional derivative, the corresponding physical energy could be obtained without the need of a line integral,<sup>61,62</sup> as it would be always given by the sum of the occupied KS eigenvalues.

The Kantorovich potential by eqs 11 and 12 is exactly the strong-interaction limit of the shifted potential defined by Levy and Zahariev. To see this, consider that the maximizing potential  $u(\mathbf{r})$  in eq 12 yields the functional  $V_{\text{ee}}^{\text{SCE}}[\rho]$  by integration

$$V_{\text{ee}}^{\text{SCE}}[\rho] = \int u(\mathbf{r}) \rho(\mathbf{r}) \, d\mathbf{r} \quad (33)$$

When  $V_{\text{ee}}^{\text{SCE}}[\rho]$  is used to approximate the Hxc functional, its functional derivative, which can be obtained exactly from eq 7, is defined, as usual, up to an arbitrary constant. If we choose to use the Kantorovich potential  $u(\mathbf{r})$  as functional derivative, the constant is fixed by the linear constraints in the dual Kantorovich problem of eq 12. In this case, the KS SCE equations read

$$-\frac{1}{2}\nabla^2 \phi_i(\mathbf{r}) + u(\mathbf{r})\phi_i(\mathbf{r}) + v_{\text{ext}}(\mathbf{r})\phi_i(\mathbf{r}) = \epsilon_i \phi_i(\mathbf{r}) \quad (34)$$

By multiplying from the left both sides of eq 34 by  $\phi_i^*(\mathbf{r})$ , integrating over  $\mathbf{r}$  and summing all the equations for the occupied orbitals, we obtain

$$T_s[\rho] + \int u(\mathbf{r}) \rho(\mathbf{r}) \, d\mathbf{r} + \int v_{\text{ext}}(\mathbf{r}) \rho(\mathbf{r}) \, d\mathbf{r} = \sum_i \epsilon_i \quad (35)$$

By virtue of eq 33, we see that the left-hand side of eq 35 gives the physical energy in the approximation  $V_{\text{ee}}^{\text{SCE}}[\rho] \approx E_{\text{Hxc}}[\rho]$ .

The constant  $C[\rho]$  has also a very clear physical meaning in the strong-interaction limit. Consider the Hamiltonian of the standard DFT adiabatic connection

$$\hat{H}^\lambda = \hat{T} + \lambda \hat{V}_{\text{ee}} + \hat{V}^\lambda \quad (36)$$

where the multiplicative one-body potential  $\hat{V}^\lambda = \sum_i v^\lambda(\mathbf{r}_i)$  enforces the density constraint in eq 1. When  $\lambda \rightarrow \infty$ , we have<sup>8,9</sup>

$$\hat{H}^{\lambda \rightarrow \infty} = \lambda(\hat{V}_{\text{ee}} + \hat{V}_{\text{SCE}}) \quad (37)$$

The corresponding classical Hamiltonian  $\hat{V}_{\text{ee}} + \hat{V}_{\text{SCE}}$  defines a classical electrostatic problem with a degenerate minimum, given by the subspace parametrized by the comotion functions. The total energy of the system in this case is exactly  $NC[\rho]$ ,

where  $N$  is the number of electrons. In other words, in the  $\lambda \rightarrow \infty$  limit, we have

$$C[\rho] = \frac{1}{N} \lim_{\lambda \rightarrow \infty} \frac{\langle \Psi^\lambda[\rho] | \hat{H}^\lambda | \Psi^\lambda[\rho] \rangle}{\lambda} \quad (38)$$

so that  $C[\rho]$  is the total electrostatic energy per electron. Since the minimum of the Hamiltonian of eq 37 is degenerate, we only need one configuration of the 3D subspace parametrized by the comotion functions (only one value of  $\mathbf{r}$ ) to compute  $C[\rho]$ . For example, in the  $N = 2$  case considered here we can choose to compute  $C[\rho]$  from the configuration corresponding to  $\mathbf{r} = \mathbf{0}$ . In this case, the second electron in the system is at infinity, so that there is no electron–electron contribution and we obtain  $C[\rho] = (1/2)v_{\text{SCE}}(\mathbf{0})$ .

From the scaling properties of the exact Hartree-exchange-correlation (Hxc) energy functional,<sup>63,64</sup> we have that if we define  $\rho_\gamma(\mathbf{r}) = \gamma^3 \rho(\gamma \mathbf{r})$ , with  $\gamma > 0$ , then<sup>10,49</sup>  $E_{\text{Hxc}}[\rho_{\gamma \rightarrow 0}] \rightarrow V_{\text{ee}}^{\text{SCE}}[\rho_\gamma]$ . Equation 38 then provides a constraint for building approximations to  $C[\rho]$ .

## 8. CONCLUSIONS AND PERSPECTIVES

In this work we have used the Kantorovich dual formulation to compute the hydrogen molecule dissociation curve using the strong interaction limit of DFT as an approximation for the exchange-correlation functional (KS SCE approach). Since the KS SCE energies are, as expected,<sup>15,17</sup> way too low around equilibrium, we have explored corrections beyond the KS SCE method. It turned out that a simple LDA correction to KS SCE performs very poorly, yielding energies that are higher than Hartree–Fock ones. It is for that reason that we considered two different nonlocal corrections to KS SCE. The inclusion of such corrections improves the overall accuracy of KS SCE, although further improvements are still needed. The main ingredient of the corrections is the comotion functions computed from the SCE potential, using an exact relation between the potential and the optimal map. The challenge is to generalize KS SCE and its corrections to larger molecular systems. For diatomics, we can still try to optimize the algorithm of the method presented in this work, but for larger systems we will probably need to approximate the SCE part, although recent promising work from the optimal transport community could yield eventually efficient SCE algorithms.<sup>37,38</sup>

Another way to use the SCE information in the construction of approximate functionals is by interpolating locally between the weak and the strong-interaction limits of DFT. We touched upon this approach and computed the SCE energy densities for  $\text{H}_2$  in the “gauge” of the electrostatic potential of the xc hole. Previously, the SCE energy densities in this “gauge” were available only for spherically symmetric systems. This information, combined with exact or approximate local quantities from the weak-interaction limit, will allow us to test different interpolation models locally. A crucial, missing ingredient for this approach is a *local* indicator of correlation (in the right “gauge”), to determine the slope around  $\lambda = 0$  of the local adiabatic connection curve. This local indicator will be first obtained in an exact way using the Legendre transform algorithms<sup>44</sup> and then approximated. This study is the object of our ongoing work.

We also showed that in the Kantorovich dual formulation, the constant in the Kohn–Sham potential recently introduced by Levy and Zahariev<sup>27</sup> arises very naturally, with a physically transparent meaning.

## APPENDIX

### A. Analytical Expressions for $\int \rho(\mathbf{r}) v_{\text{SCE}}(\mathbf{r}) d\mathbf{r}$

With the parametrizations of  $v_{\text{SCE}}(\mathbf{r})$  of eq 18 and of  $\rho(\mathbf{r})$  of eq 19, the integral  $\int \rho(\mathbf{r}) v_{\text{SCE}}(\mathbf{r}) d\mathbf{r}$  becomes

$$\int_0^{2\pi} d\theta \int_{-\infty}^{\infty} dz \int_0^{\infty} h dh v(z, h) \rho(z, h) \\ = 2\pi^{3/2} \sum_{i=1}^m \sum_{j=1}^Q \alpha_j \left( \frac{A_i e^{-\beta_j^2 p_i \gamma_j^2 / \beta_j^2 + p_i}}{\sqrt{\beta_j^2 + p_i} (\beta_j^2 + q_i)} + \frac{\text{erf}\left(\frac{a\beta_j \gamma_j}{\sqrt{a^2 + \beta_j^2}}\right)}{\beta_j^3 \gamma_j} \right) \quad (39)$$

## AUTHOR INFORMATION

### Corresponding Author

\*E-mail: p.gorigiorgi@vu.nl

### Notes

The authors declare no competing financial interest.

## ACKNOWLEDGMENTS

This work was supported by the Netherlands Organization for Scientific Research (NWO) through an ECHO grant (717.013.004) and a Vidi grant (700.59.428).

## REFERENCES

- (1) Kohn, W.; Sham, L. J. *Phys. Rev.* **1965**, *140*, 1133.
- (2) Cohen, A. J.; Mori-Sánchez, P.; Yang, W. *Chem. Rev.* **2012**, *112*, 289.
- (3) Becke, A. D. *J. Chem. Phys.* **2014**, *140*, 18A301.
- (4) Cramer, C. J.; Truhlar, D. G. *Phys. Chem. Chem. Phys.* **2009**, *11*, 10757.
- (5) Perdew, J. P.; Ruzsinszky, A.; Tao, J.; Staroverov, V. N.; Scuseria, G. E.; Csonka, G. I. *J. Chem. Phys.* **2005**, *123*, 062201.
- (6) Peverati, R.; Truhlar, D. G. *Philos. Trans. R. Soc. London, Ser. A* **2014**, *372*, 20120476.
- (7) Seidl, M. *Phys. Rev. A* **1999**, *60*, 4387.
- (8) Seidl, M.; Gori-Giorgi, P.; Savin, A. *Phys. Rev. A* **2007**, *75*, 042511.
- (9) Gori-Giorgi, P.; Vignale, G.; Seidl, M. *J. Chem. Theory Comput.* **2009**, *5*, 743.
- (10) Malet, F.; Gori-Giorgi, P. *Phys. Rev. Lett.* **2012**, *109*, 246402.
- (11) Malet, F.; Mirschink, A.; Cremon, J. C.; Reimann, S. M.; Gori-Giorgi, P. *Phys. Rev. B* **2013**, *87*, 115146.
- (12) Mendl, C. B.; Malet, F.; Gori-Giorgi, P. *Phys. Rev. B* **2014**, *89*, 125106.
- (13) Mirschink, A.; Seidl, M.; Gori-Giorgi, P. *Phys. Rev. Lett.* **2013**, *111*, 126402.
- (14) Kurth, S.; Stefanucci, G. *Phys. Rev. Lett.* **2013**, *111*, 030601.
- (15) Chen, H.; Friesecke, G.; Mendl, C. B. *J. Chem. Theory Comput.* **2014**, *10*, 4360–4368.
- (16) Wagner, L. O.; Stoudenmire, E. M.; Burke, K.; White, S. R. *Phys. Chem. Chem. Phys.* **2012**, *14*, 8581.
- (17) Malet, F.; Mirschink, A.; Giesbertz, K.; Wagner, L.; Gori-Giorgi, P. *Phys. Chem. Chem. Phys.* **2014**, *16*, 14551–14558.
- (18) Mirschink, A.; Umrigar, C. J.; Morgan, J. D.; Gori-Giorgi, P. *J. Chem. Phys.* **2014**, *140*, 18A532.
- (19) Wagner, L. O.; Gori-Giorgi, P. *Phys. Rev. A* **2014**, *90*, 052512.
- (20) Buttazzo, G.; De Pascale, L.; Gori-Giorgi, P. *Phys. Rev. A* **2012**, *85*, 062502.
- (21) Cotar, C.; Friesecke, G.; Klüppelberg, C. *Comm. Pure Appl. Math.* **2013**, *66*, 548.
- (22) Mendl, C. B.; Lin, L. *Phys. Rev. B* **2013**, *87*, 125106.

- (23) Friesecke, G.; Mendl, C. B.; Pass, B.; Cotar, C.; Klüppelberg, C. *J. Chem. Phys.* **2013**, *139*, 164109.
- (24) Monge, G. *Mémoire sur la théorie des déblais et des remblais*; Histoire Acad. Sciences: Paris, 1781.
- (25) Kantorovich, L. V. *Dokl. Akad. Nauk. SSSR.* **1942**, *37*, 227.
- (26) Villani, C. *Topics in Optimal Transportation*; American Mathematical Society: Providence, RI, 2003; Grad. Stud. Math. 58.
- (27) Levy, M.; Zahariev, F. *Phys. Rev. Lett.* **2014**, *113*, 113002.
- (28) Harris, J. *Phys. Rev. A* **1984**, *29*, 1648.
- (29) Langreth, D. C.; Perdew, J. P. *Solid State Commun.* **1975**, *17*, 1425.
- (30) Levy, M. *Proc. Natl. Acad. Sci. U.S.A.* **1979**, *76*, 6062.
- (31) Seidl, M.; Perdew, J. P.; Levy, M. *Phys. Rev. A* **1999**, *59*, 51.
- (32) Mirschink, A.; Seidl, M.; Gori-Giorgi, P. *J. Chem. Theory Comput.* **2012**, *8*, 3097.
- (33) Gori-Giorgi, P.; Seidl, M.; Vignale, G. *Phys. Rev. Lett.* **2009**, *103*, 166402.
- (34) Liu, Z. F.; Burke, K. *J. Chem. Phys.* **2009**, *131*, 124124.
- (35) Colombo, M.; De Pascale, L.; Di Marino, S. *Can. J. Math.* **2015**, *67*, 350.
- (36) Lieb, E. H. *Int. J. Quantum Chem.* **1983**, *24*, 24.
- (37) Benamou, J.-D.; Carlier, G.; Cuturi, M.; Nenna, L.; Peyré, G. *Iterative Bregman Projections for Regularized Transportation Problems*; arXiv: 1412.5154, 2015.
- (38) Benamou, J.-D.; Carlier, G.; Nenna, L. *A Numerical Method to solve Optimal Transport Problems with Coulomb Cost*; arXiv: 1505.01136v2, 2015.
- (39) Helbig, N.; Tokatly, I. V.; Rubio, A. *J. Chem. Phys.* **2009**, *131*, 224105.
- (40) Buijse, M. A.; Baerends, E. J.; Snijders, J. G. *Phys. Rev. A* **1989**, *40*, 4190.
- (41) Mori-Sánchez, P.; Cohen, A. J.; Yang, W. *Phys. Rev. Lett.* **2008**, *100*, 146401.
- (42) Schmidt, M. W.; Baldrige, K. K.; Boatz, J. A.; Elbert, S. T.; Gordon, M. S.; Jensen, J. J.; Koseki, S.; Matsunaga, N.; Nguyen, K. A.; Su, S.; Windus, T. L.; Dupuis, M.; Montgomery, J. A. *J. Comput. Chem.* **1993**, *14*, 1347.
- (43) Dunning, T. H. *J. Chem. Phys.* **1989**, *90*, 1007.
- (44) Teale, A. M.; Coriani, S.; Helgaker, T. *J. Chem. Phys.* **2009**, *130*, 104111.
- (45) Lewin, M.; Lieb, E. H. *Phys. Rev. A* **2015**, *91*, 022507.
- (46) Fuchs, M.; Niquet, Y. M.; Gonze, X.; Burke, K. *J. Chem. Phys.* **2005**, *122*, 094116.
- (47) Achan, D.; Massa, L.; Sahni, V. *Phys. Rev. A* **2014**, *90*, 022502.
- (48) Gritsenko, O. V.; van Leeuwen, R.; Baerends, E. J. *J. Chem. Phys.* **1997**, *104*, 8535.
- (49) Gori-Giorgi, P.; Seidl, M. *Phys. Chem. Chem. Phys.* **2010**, *12*, 14405.
- (50) Ernzerhof, M. *Chem. Phys. Lett.* **1996**, *263*, 499.
- (51) Burke, K.; Ernzerhof, M.; Perdew, J. P. *Chem. Phys. Lett.* **1997**, *265*, 115.
- (52) Becke, A. D. *J. Chem. Phys.* **1993**, *98*, 5648.
- (53) Mori-Sánchez, P.; Cohen, A. J.; Yang, W. T. *J. Chem. Phys.* **2006**, *124*, 091102.
- (54) Liu, Z. F.; Burke, K. *Phys. Rev. A* **2009**, *79*, 064503.
- (55) Gori-Giorgi, P.; Savin, A. *J. Phys.: Conf. Ser.* **2008**, *117*, 012017.
- (56) Savin, A. *Chem. Phys.* **2009**, *356*, 91.
- (57) Becke, A. D. *J. Chem. Phys.* **2005**, *122*, 064101.
- (58) Perdew, J. P.; Staroverov, V. N.; Tao, J.; Scuseria, G. E. *Phys. Rev. A* **2008**, *78*, 052513.
- (59) Lammert, P. E. *Int. J. Quantum Chem.* **2007**, *107*, 1943–1953.
- (60) Kvaal, S.; Ekstöm, U.; Teale, A. M.; Helgaker, T. *J. Chem. Phys.* **2014**, *140*, 18A518.
- (61) Gaiduk, A. P.; Chulkov, S. K.; Staroverov, V. N. *J. Chem. Theory Comput.* **2009**, *5*, 699–707.
- (62) van Leeuwen, R.; Baerends, E. J. *Phys. Rev. A* **1995**, *51*, 170.
- (63) Levy, M.; Perdew, J. P. *Phys. Rev. A* **1985**, *32*, 2010.
- (64) Levy, M.; Perdew, J. P. *Phys. Rev. B* **1993**, *48*, 11638.